

Geometric Fourier Analysis of the Conformal Camera for Active Vision*

Jacek Turski[†]

Abstract. Suppose one intends to design an active vision system that should perform some artificial intelligence functions. For instance, it should recognize a planar object (or a three-dimensional object containing a piece of a planar surface) in a dynamic scene. Ideally, such a system should be built upon some data model representing visual inputs and algorithms storing, processing, and analyzing visual information that are well adapted to image transformations produced by different perspectives between planar objects and the imaging system. In spite of its importance, this problem remained unsolved until recently. In this article, building on the author's work, projective Fourier analysis for patterns is constructed in the framework of geometric Fourier analysis on groups and homogeneous spaces. It is done by identifying in the conformal camera the group $\mathbf{SL}(2, \mathbb{C})$, which gives image projective transformations by acting through linear-fractional mappings on the image plane—homogeneous under the group action. This analysis is being implemented in perspectively adapted digital image processing, and its basic components are tested for binary images in computer simulations. It is recognized that the data model of digital image representation developed in the article is explicitly designed for foveated sensors, the use of which in active vision systems is presently limited due to the lack of such a data model.

Key words. irreducible unitary representations of Lie groups, geometric Fourier analysis, the conformal camera, projective Fourier analysis, perspectively adapted image processing, retinotopic mapping, foveated vision

AMS subject classifications. 43A30, 43A65, 43A85, 51N30, 68T10, 68U10

DOI. 10.1137/S0036144502400961

I. Introduction. A long-standing goal in imaging science is to develop image representation and efficient algorithms for storing, processing, and rendering visual information that are well adapted to the types of geometric transformations dictated by a problem at hand. These developments can be categorized into two distinct, although interrelated, groups. One group is based on the geometric approach, and the other on the imaging approach. The geometric approach begins with the representation of shapes of objects in terms of geometrical primitives (mathematical abstractions), such as lines, polygons, splines, and spheres; theorems from analytical geometry (Euclidean, affine, or projective) are of paramount importance [31, 32, 39]. The imaging approach, on the other hand, deals with the image data given or extracted in terms of arrays of numbers—discrete samples of pixels—frequently coming

*Received by the editors January 14, 2002; accepted for publication (in revised form) October 31, 2003; published electronically May 3, 2004. This work was supported in part by NSF grant CCR-9901957.

<http://www.siam.org/journals/sirev/46-2/40096.html>

[†]Department of Computer and Mathematical Sciences, University of Houston-Downtown, One Main Street, Houston, TX 77002-1001 (turskij@uhd.edu).

from nongeometrical sources such as magnetic resonance imaging recordings. Here the harmonic analysis with Fourier, Gabor, or wavelet theories and the sampling theorem are of paramount importance [1, 6, 11, 13, 28, 29]. Also see [10] for the newest innovations in computational harmonic analysis, especially promising in natural scene statistics (NSS) research. The geometric approach is more common for problems in computer vision (robotics and industrial inspections, for example) and computer graphics (image-based modeling and rendering and visual art, for example), while the imaging approach is more common for problems such as resilient watermarking, content-based image retrieval, and modeling primate visual systems in neuroscience (retinocortical image transformation and cortical image coding and analyzing).

An active vision system consisting of a moving camera head coupled with a hardware image processor and linked to the computer performing image analysis should be built upon the data model representing visual inputs and efficient algorithms processing and analyzing visual information that is well adapted to image projective transformations produced by different perspectives between objects and the camera. A substantial amount of work done on the construction of an active vision system (the one we have described above or with more specialized functions) using the geometrical approach has not been successful so far. A more general discussion in [30] on whether mathematical theories of shape could provide the right approach to active vision problems yielded a pessimistic outcome. The imaging approach, on the other hand, that deals with the data model (analog or digital) of image representation based on harmonic analysis, although more promising, suffers from the lack of projective covariance. It is well known that all the theories of harmonic analysis mentioned above are not well adapted to image perspective transformations. For example, one can efficiently reconstruct a pattern that is rotated and translated in an image plane using only one Fourier transform of the original pattern; but when perspective transformations are applied, this is no longer feasible. These facts can be understood if one realizes that the Fourier, Fourier–Mellin, wavelet, and Gabor transforms are built on Euclidean, similarities, affine, and Weyl–Heisenberg (sub)groups of transformations, respectively. Thus, one should look for an extension of the transforms that could be built on some projective group. This leads naturally to the subject of Lie group representations, and in particular to geometric Fourier analysis.

A substantial amount of work has been done to develop image representations along the lines of Lie group theory that provide invariant and/or covariant descriptions under image transformations by the important Lie groups of rigid motions, similarities, and some projected motion groups; see, for example, [2, 4, 14, 16, 17, 38]. However, only recently, the data model of the digital image representation based on projective Fourier analysis for patterns (i.e., *planar* objects) constructed in the framework of Lie group representations has been developed in a series of papers [41, 42, 43, 45]. Especially promising in this development is the fact that projective Fourier analysis provides the data model for digital image representation that is explicitly designed for the foveated architecture of silicon retina sensors used in some cameras (see [46] on the SIAM-MI03 conference in Toronto), the use of which in active vision systems is presently limited due to the lack of such a model [48].

The main idea of the theory of group representations in their relation to geometric Fourier analysis is to decompose a function space on a group, or on a set on which the group acts naturally, in terms of the *simplest* homomorphisms of the group, into the set of unitary linear operators on a Hilbert space, called irreducible unitary representations. In this framework, the generalized Fourier transform plays the same role

on any group as the classical Fourier transform on the additive group of real numbers, where the irreducible unitary representations are homomorphisms between the additive group and the multiplicative group of complex numbers of modulus 1 (the circle group), given by the complex exponential functions one finds in the definition of the standard Fourier integral. Since group theory is rooted in large part in geometry through Klein's Erlanger program of studying spaces through their groups of motions, this geometric Fourier analysis emphasizes from the very beginning the covariance, with respect to the geometric transformations, of the decompositions.

In this article, building on the author's previous work, we discuss projective Fourier analysis in a carefully laid framework of geometric Fourier analysis: given geometric action of the group \mathbf{G} on the space X (in our work, the projective group \mathbf{G} acting on the image plane), decompose some natural unitary representations \mathcal{T} of \mathbf{G} on the Hilbert space $L^2(X)$ of square-integrable functions on X (patterns of finite energy) into their irreducible constituents present in this space. Then we develop digital image processing based on projective Fourier decomposition of patterns and numerically test its basic components for binary images. Although it has been said (see the comments in section 7 of [19]) that there is no royal road through contemporary (semisimple) harmonic analysis, including infinite-dimensional representation theory, the exposition given here is intended for a broad audience, including scientists working in computer vision, computer graphics, image processing, and computational neuroscience. Therefore, we give all necessary definitions, illustrating examples, and explicit calculations, as well as stressing motivations and nontechnical explanations.

The article is organized as follows: In the next section, after we introduce basic facts of representation theory, the above-mentioned geometric Fourier analysis on $L^2(X)$ is more precisely formulated. Then, in section 3, we work out two examples related to the group of Euclidean geometry, to illustrate the mathematical framework of geometric Fourier analysis.

In section 4 we introduce the projective camera model for patterns. The group $\mathbf{SL}(2, \mathbb{C})$ of 2×2 complex matrices of determinant 1, identified in this camera, acts by linear-fractional (conformal) mappings on the image plane homogeneous under the group action, giving image projective transformations. We also mention the camera's *conformal lens optics*, which is caused by the way rotations are generated. Having identified the projective group $\mathbf{SL}(2, \mathbb{C})$, in the next section we discuss Gauss and Iwasawa decompositions of $\mathbf{SL}(2, \mathbb{C})$ and give the corresponding integral formulas, which are used in section 6 to obtain the irreducible unitary representations in the L^2 -space in the so-called noncompact picture of induced representation. These representations provide the building blocks in the construction given in section 7 of geometric Fourier analysis on the image plane, homogeneous under the group $\mathbf{SL}(2, \mathbb{C})$. It consists of the projective Fourier transform (PFT), its inverse, and the Plancherel theorem. Section 8 discusses the derivation of the discrete projective Fourier transform (DPFT) and its inverse from the corresponding continuous transforms, stressing numerical aspects.

Next, in section 9, we develop the analytical foundations of the digital image processing based upon DPFT. Since DPFT has the form of the standard discrete Fourier transform in log-polar coordinates, it can be computed by a two-dimensional fast Fourier transform (FFT). Accordingly, we discuss the *sampling interface*: the procedure under which a uniformly sampled image is resampled with a log-polar sampling—a nonuniform scheme of sampling—and again becomes uniform by being expressed in the log-polar coordinate plane. The projective Fourier representation of a digital pattern allows one to render its image projective transformations by computing

only the DPFT of the original pattern. However, conformal distortions caused by the conformal lens optics of the camera must be removed from image projective transformations in order to display image perspective transformations. We address this problem, which is referred to as the *deconformalization problem*, in this section as well. We conclude this section by recognizing that the DPFT provides the right computational framework for developing elegant image processing tools explicitly designed for the foveated, or space-variant, architecture of silicon retina sensors. Finally, in section 10 we carry out computer simulations to test the projective covariance of the image representation for binary digital images.

Fourier analysis on homogeneous spaces, and on symmetric spaces in particular, based on geometric ideas was originated by Gelfand’s school and by Harish-Chandra, and further developed by Helgason [20, 21]. Although we work with geometric Fourier analysis of $\mathbf{SL}(2, \mathbb{C})$, that is, harmonic analysis for the simplest noncompact semisimple complex Lie group (developed by Gelfand’s school [15]), it is preferable to present the basic methods of representation theory and harmonic analysis in the more general context of semisimple Lie groups (Harish-Chandra’s approach). For the definition of a semisimple Lie group in the context used in this work, we refer to [24], where an elementary account of Harish-Chandra’s fundamental (but very technical) work in the field of representation theory is also given. A good introduction to the field of representation theory of semisimple Lie groups can be found in [27]. Nontechnical expositions on the connection between group representations and geometric Fourier analysis were given in [19, 35]. The former includes a historical perspective, and the latter, a detailed discussion of the $\mathbf{SL}(2, \mathbb{C})$ case. Special cases of geometric Fourier analysis on the two-dimensional sphere S^2 , the symmetric space of the rotation group $\mathbf{SO}(3)$, and non-Euclidean analogs of Fourier series and integrals with many applications, were discussed in [40].

Finally, we mention that the presentation of projective Fourier analysis given in sections 2–8 of this article is an expanded version of a seminar given by the author in June 2001 at City University of Hong Kong [44].

2. Basic Facts of Representation Theory. We shall mostly be concerned with groups \mathbf{G} , which are matrix Lie groups, that is, closed subgroups of the groups of invertible $n \times n$ matrices with real or complex entries. A manifold X is a transformation space for a group \mathbf{G} if there is a continuous action $\mathbf{G} \times X \rightarrow X$, $(g, x) \mapsto g \cdot x$ such that $g \cdot (h \cdot x) = (gh) \cdot x$ and $e \cdot x = x$ for all $x \in X$ and $g, h \in \mathbf{G}$, where e is the identity element of \mathbf{G} . We shall assume that the action is transitive, which means that given $x, y \in X$, there is a $g \in \mathbf{G}$ such that $y = g \cdot x$. In this case the space X is called a *homogeneous space*. A transformation space X for \mathbf{G} is a homogeneous space if and only if X is isomorphic to \mathbf{G}/\mathbf{H} , where \mathbf{H} is the isotropy group $\mathbf{G}_x = \{g \mid g \cdot x = x\}$ of any designated point $x \in X$.

A *representation of a group* \mathbf{G} on a vector space H , usually assumed complex, is a homomorphism $\mathcal{T} : \mathbf{G} \rightarrow \mathbf{GL}(H)$ from \mathbf{G} to the space $\mathbf{GL}(H)$ of invertible linear operators on H , that is, $\mathcal{T}(gh) = \mathcal{T}(g)\mathcal{T}(h)$ and $\mathcal{T}(g^{-1}) = \mathcal{T}^{-1}(g)$ for all $g, h \in \mathbf{G}$. Therefore, if H is a topological vector space, a representation \mathcal{T} is obtained from the action $(g, v) \mapsto \mathcal{T}(g)v$ that is linear in v . Although we consider only the matrix Lie groups, it does not mean that the vector space on which the representation of \mathbf{G} acts is finite-dimensional. If the vector space H has a finite dimension, the degree of the representation \mathcal{T} is the dimension of the vector space H . Otherwise, we say that \mathcal{T} is an infinite-dimensional representation. A representation is said to be *unitary* if H is a Hilbert space with an inner product $\langle v, u \rangle$, and each $\mathcal{T}(g)$ is a unitary operator

in H ; that is, the inner product is invariant,

$$\langle \mathcal{T}(g)v, \mathcal{T}(g)u \rangle = \langle v, u \rangle,$$

for all $g \in \mathbf{G}$ and $v, u \in H$. Because we are working with geometric Fourier analysis, we shall present the basic facts for unitary representations only.

If H is a Hilbert space, a representation is a homomorphism $\mathcal{T} : \mathbf{G} \rightarrow \mathbf{BL}(H)$ from \mathbf{G} to the space of linear operators on H with bounded inverses, such that the resulting map $\mathbf{G} \times H \rightarrow H$ is continuous. To have this continuity for unitary representations it is enough to assume that the function $g \rightarrow \langle \mathcal{T}(g)v, v \rangle$ is continuous at $g = e$ for all $v \in H$.

A representation \mathcal{T}_1 of \mathbf{G} on H_1 is said to be *equivalent* to a representation \mathcal{T}_2 on H_2 if there exists a bounded isomorphism $S : H_1 \rightarrow H_2$ such that $S\mathcal{T}_1(g) = \mathcal{T}_2(g)S$ for all $g \in \mathbf{G}$. In addition, if $S : H_1 \rightarrow H_2$ is a unitary isomorphism, the representations are *unitarily equivalent*. We regard equivalent representations as being essentially the same.

A representation can be restricted to a closed subgroup, or different representations can be combined, to yield the new representations. An important example, when two representations are combined, is the case of the direct sum. Let two representations of \mathbf{G} , \mathcal{T}_1 on H_1 and \mathcal{T}_2 on H_2 , be given. If $H_1 \oplus H_2$ is the direct sum of the Hilbert spaces, that is, it consists of all vectors $(v_1, v_2) \in H_1 \times H_2$ with the scalar product being componentwise,

$$\langle (v_1, v_2), (w_1, w_2) \rangle_{H_1 \oplus H_2} = \langle v_1, w_1 \rangle_{H_1} + \langle v_2, w_2 \rangle_{H_2},$$

then the direct sum representation $\mathcal{T}_1 \oplus \mathcal{T}_2$ of \mathbf{G} on $H_1 \oplus H_2$ is defined as follows:

$$v_1 \oplus v_2 \mapsto \mathcal{T}_1 \oplus \mathcal{T}_2(g)(v_1, v_2) = (\mathcal{T}_1(g)v_1, \mathcal{T}_2(g)v_2).$$

Let \mathcal{T} be a representation of \mathbf{G} on a Hilbert space H . A closed subspace $W \subset H$ is said to be invariant (with respect to \mathcal{T}) if $\mathcal{T}(g)W \subset W$ for all $g \in \mathbf{G}$. In this case, the representation \mathcal{T} reduces to a subrepresentation of \mathbf{G} on W .

Every representation has at least two trivial subrepresentations, namely, when $W = \{0\}$ and $W = H$. A *reducible* representation is one that contains a nontrivial subrepresentation; an *irreducible* representation, then, is one that has no nontrivial subrepresentations.

When a representation \mathcal{T} of \mathbf{G} on H is reducible, with a closed invariant subspace W , we can ask whether we can find an invariant subspace W' such that $H = W \oplus W'$. In general it cannot be done. However, if the representation \mathcal{T} is unitary, the invariance of the inner product $\langle \mathcal{T}(g)v_1, \mathcal{T}(g)v_2 \rangle = \langle v_1, v_2 \rangle$ for all $g \in \mathbf{G}$ and $v_1, v_2 \in H$ implies that W is invariant if and only if

$$W^\perp = \{v \in H \mid \langle v, u \rangle = 0 \text{ for all } u \in W\}$$

is invariant, and $H = W \oplus W^\perp$. In particular, finite-dimensional unitary representations are always direct sums of irreducibles.

The following simple proposition, referred to as *Schur's lemma*, often proves crucial.

PROPOSITION 1. *If representations \mathcal{T}_1 and \mathcal{T}_2 of \mathbf{G} on H_1 and H_2 , respectively, are finite-dimensional and irreducible, then any linear map $F : H_1 \rightarrow H_2$ such that $F(\mathcal{T}_1(g)v) = \mathcal{T}_2(g)F(v)$ is either zero or an isomorphism. Furthermore, if $H_1 = H_2$, then $F = \lambda Id$ for some $\lambda \in \mathbb{C}$.*

The proposition holds because the subspaces $\ker(F) \subset H_1$, $\text{im}(F) \subset H_2$, and (if $H_1 = H_2$) any eigenspace $\{v \in H \mid F(v) = \lambda v\}$ are all invariant subspaces and consequently are either $\{0\}$ or coincide with the entire space by the definition of irreducibility.

The infinite-dimensional extension of the last proposition holds for the unitary representations. This fundamental result in representation theory is also referred to as (generalized) *Schur's lemma*.

THEOREM 2. *Let \mathcal{T}_1 and \mathcal{T}_2 be unitary, irreducible representations of \mathbf{G} on H_1 and H_2 , respectively. If $S : H_1 \rightarrow H_2$ is a bounded linear operator such that $S\mathcal{T}_1(g) = \mathcal{T}_2(g)S$ for every $g \in \mathbf{G}$, then either S is an isomorphism (i.e., \mathcal{T}_1 and \mathcal{T}_2 are equivalent: $\mathcal{T}_2 \cong \mathcal{T}_1 \iff \mathcal{T}_2(g) = S\mathcal{T}_1(g)S^{-1}$) or $S = 0$.*

The last theorem implies the following *criterion of irreducibility*: a unitary representation \mathcal{T} of \mathbf{G} on H is irreducible if and only if the only operators commuting with all $\mathcal{T}(g)$ are scalar multiples of the identity.

Given a Lie group \mathbf{G} of geometric transformations acting on a homogeneous space X , there is a naturally induced representation \mathcal{T} of \mathbf{G} on the space $F(X)$ of complex functions F on X , the representation that maps F to the function $F_g = \mathcal{T}(g)F$ defined by $F_g(x) = F(g^{-1} \cdot x)$. This representation on the (infinite-dimensional) function space F will usually decompose into many important subrepresentations, some of them finite dimensional.

EXAMPLE 3. *In this example a Lie group \mathbf{G} is acting on itself by multiplications: left multiplication $g \mapsto hg$, or right multiplication $g \mapsto gh^{-1}$, both multiplications by $h \in \mathbf{G}$. The linear space here is $H = L^2(\mathbf{G}, d_l g)$ taken with respect to a left-invariant (Haar) measure: $d_l(hg) = d_l g$ for all $h \in \mathbf{G}$. Then, $L(h)f(g) = f(h^{-1}g)$ is the left regular representation of \mathbf{G} . The right regular representation is given by $R(h)f(g) = f(gh)$ on $L^2(\mathbf{G}, d_r g)$, where $d_r g$ is a right-invariant (Haar) measure on \mathbf{G} ; $d_r(gh) = d_r g$. Both representations are unitary. We check this fact only for the left regular representation, as the case of the right regular representation can be proved along the same lines. To this end, we have*

$$\begin{aligned} \langle L(h)f_1, L(h)f_2 \rangle &= \int_{\mathbf{G}} L(h)f_1(g) \overline{L(h)f_2(g)} d_l g \\ &= \int_{\mathbf{G}} f_1(h^{-1}g) \overline{f_2(h^{-1}g)} d_l g. \end{aligned}$$

Using the left invariance in this integral, we obtain

$$\begin{aligned} \langle L(h)f_1, L(h)f_2 \rangle &= \int_{\mathbf{G}} f_1(g) \overline{f_2(g)} d_l g \\ &= \langle f_1, f_2 \rangle. \end{aligned}$$

This shows that $L(h)$ is unitary.

In this example the homogeneous space X of the group \mathbf{G} is the group itself. The constructions of the unitary representations involved the invariant (Haar) measures $d_l g$ and $d_r g$ with respect to which the invariant inner products of the corresponding L^2 -spaces were constructed. Every Lie group carries both left- and right-invariant measures $d_l g$ and $d_r g$. Although in general $d_l g$ and $d_r g$ are different, they vanish on the same null sets; that is, they are equivalent measures. Therefore, there is a measurable function $\Delta_{\mathbf{G}} : \mathbf{G} \rightarrow \mathbb{R}_+$ such that $d_r g = \Delta_{\mathbf{G}}(g)d_l g$. This function is called the *modular function* of the group \mathbf{G} . If $\Delta_{\mathbf{G}} = 1$, the group is called *unimodular*.

A homogeneous space X of the group \mathbf{G} , on the other hand, need not carry any measure invariant under the action of \mathbf{G} on X . However, a *quasi-invariant* measure $d\mu$ on X always exists, and this fact is enough to construct unitary representations of \mathbf{G} on $L^2(X, d\mu)$. The measure $d\mu$ on the homogeneous space X of the group \mathbf{G} is said to be quasi-invariant if $d\mu(x)$ and $d\mu(g \cdot x)$ are equivalent measures. In fact, the mapping $g \mapsto \mathcal{T}(g)$ given by

$$(1) \quad \mathcal{T}(g)f(x) = \sqrt{\frac{d\mu(g^{-1} \cdot x)}{d\mu(x)}} f(g^{-1} \cdot x)$$

provides a unitary representation \mathcal{T} of \mathbf{G} on $L^2(X, d\mu)$.

Now, the basic problem of geometric Fourier analysis can be formulated as follows: Given geometric action of \mathbf{G} on X , find a \mathbf{G} -equivariant isomorphism $L^2(X, d\mu) \cong \widehat{V}$, where \widehat{V} is a space built explicitly out of unitary irreducible representations in $L^2(X, d\mu)$, as a direct sum or possibly in some more general fashion. This “more general fashion” will be explained in the examples given in the next section.

3. Fourier Analysis from the Euclidean Group. In this section we present two examples of geometric Fourier analysis. The first is the classical Fourier analysis on \mathbb{R}^n , where \mathbb{R}^n is taken to be the additive group. In the second example Fourier analysis is formulated on the Euclidean space \mathbb{R}^n (we take $n = 2$ to eliminate unnecessary complications), the homogeneous space of the Euclidean group.

3.1. Classical Fourier Analysis. The Fourier transform \mathcal{F} given by the integral

$$(\mathcal{F}f)(\lambda) = \widehat{f}(\lambda) = \int_{\mathbb{R}^n} f(x)e^{-i\lambda \cdot x} dx,$$

where $\lambda \cdot y$ denotes the standard inner product on \mathbb{R}^n , is first defined on $L^1(\mathbb{R}^n) \cap L^2(\mathbb{R}^n)$ and is then extended to an *isometry* on $L^2(\mathbb{R}^n)$ that satisfies the *Plancherel formula*:

$$\int_{\mathbb{R}^n} |f(x)|^2 dx = \frac{1}{(2\pi)^n} \int_{\mathbb{R}^n} |\widehat{f}(\lambda)|^2 d\lambda.$$

Its inverse Fourier transform \mathcal{F}^{-1} , given by

$$\left(\mathcal{F}^{-1}\widehat{f}\right)(x) = f(x) = \frac{1}{(2\pi)^n} \int_{\mathbb{R}^n} \widehat{f}(\lambda)e^{i\lambda \cdot x} d\lambda,$$

provides the decomposition of functions in the L^2 sense.

This classical harmonic analysis is in fact geometric Fourier analysis on the abelian group $\mathbf{G} = \mathbb{R}^n$ acting by translations on the Euclidean space \mathbb{R}^n . The regular (unitary) representation

$$(\mathcal{T}(y)f)(x) = f(x - y), \quad f \in L^2(\mathbb{R}^n),$$

decomposes into (one-dimensional) irreducible unitary representations $\pi_\lambda(y) = e^{i\lambda \cdot y}$.

Although all irreducibles must be one-dimensional since the group is abelian, the Hilbert space $L^2(\mathbb{R}^n)$ does not contain one-dimensional invariant subspaces since $c\pi_\lambda \notin L^2(\mathbb{R}^n)$. However, there is an invariant (Plancherel’s) measure on the set of

equivalent classes of irreducible unitary representations $\widehat{\mathbb{R}^n}$, isomorphic to \mathbb{R}^n (under the correspondence $\pi_\lambda \leftrightarrow \lambda$), namely, $d\rho(\lambda) = (1/(2\pi)^n) d\lambda$. Writing

$$\mathcal{T} \cong \widehat{\mathcal{T}} = \mathcal{F}\mathcal{T}\mathcal{F}^{-1} = \int_{\mathbb{R}^n}^{\oplus} \pi_\lambda d\rho(\lambda)$$

(\mathcal{T} and $\widehat{\mathcal{T}} = \mathcal{F}\mathcal{T}\mathcal{F}^{-1}$ are equivalent representations since \mathcal{F} is a unitary isomorphism) and

$$L^2(\mathbb{R}^n) = \int_{\mathbb{R}^n}^{\oplus} \mathbb{C}\pi_\lambda d\rho(\lambda),$$

we can think of them as a *continuous direct sum*, or *direct integral* of irreducible representations π_λ ; see [19]. This can be made precise in the framework of the theory of spectral decomposition of operators. However, it will not be needed in our applications to image processing as we will work with the DPFT.

3.2. Euclidean Fourier Analysis. The Euclidean group $\mathbf{E}(2) = \mathbf{SO}(2) \rtimes \mathbb{R}^2$ is the semidirect product of the group of rotations about the origin and the group of translations. We identify $\mathbf{E}(2)$ with the group of matrices $g = \begin{pmatrix} e^{i\varphi} & \xi \\ 0 & 1 \end{pmatrix}$ acting on the quotient space $X = \mathbf{E}(2)/\mathbf{SO}(2) \cong \mathbb{R}^2$, which is regarded here as \mathbb{C} , as follows: $g \cdot z = e^{i\varphi}z + \xi$. For each real number $s \neq 0$, H_s is the Hilbert space of functions on \mathbb{C} ,

$$f(z) = \int_{S^1} F(\omega) e^{is \operatorname{Re}(\bar{z}\omega)} d\omega, \quad F(\omega) \in L^2(S^1),$$

where $d\omega$ is the invariant measure, and with the norm given by

$$\|f\| = \left(\int_{S^1} |F(\omega)|^2 d\omega \right)^{1/2}.$$

The regular representations of $\mathbf{E}(2)$ on H_s , $s > 0$,

$$\mathcal{T}_s(g)f(z) = f(g^{-1} \cdot z) = f(e^{-i\varphi}(z - \xi)),$$

are all of the unequivalent *infinite-dimensional* unitary and irreducible representations [20]. In order to derive the Euclidean Fourier transform, we first write the Fourier transform $\mathcal{F}f = \widehat{f}$ in polar coordinates,

$$\widehat{f}(s\omega) = \frac{i}{2} \int_{\mathbb{C}} f(z) e^{-is \operatorname{Re}(\bar{z}\omega)} dz d\bar{z}, \quad f \in L^2(\mathbb{C}),$$

where if $z = x + iy$, then $(i/2)dzd\bar{z} = dx dy$. Next, for every $f \in C_c^\infty(\mathbb{C})$, we have

$$f(z) = \frac{1}{2\pi} \int_{\mathbb{R}_+} \int_{S^1} \widehat{f}(s\omega) e^{is \operatorname{Re}(\bar{z}\omega)} d\omega ds.$$

Then the regular representation of $\mathbf{E}(2)$ on $L^2(\mathbb{C})$, $\mathcal{T}(g)f(z) = f(g^{-1} \cdot z)$, has the spectral decomposition into irreducibles

$$\mathcal{T} \cong \widehat{\mathcal{T}} = \mathcal{F}\mathcal{T}\mathcal{F}^{-1} = \int_{\mathbb{R}_+}^{\oplus} \mathcal{T}_s ds$$

and

$$L^2(\mathbb{C}) = \int_{\mathbb{R}_+}^{\oplus} H_s s ds.$$

Finally, writing $\omega = e^{i\phi}$ and $z = re^{i\theta}$ and using elementary properties of the classical Fourier transform, any $f \in L^2(\mathbb{C})$ has the Euclidean Fourier decomposition in terms of *Bessel functions* J_n :

$$f(z) = \frac{1}{2\pi} \sum_{n=-\infty}^{n=\infty} \int_{\mathbb{R}_+} \widehat{f}(n, s) \left(\frac{z}{|z|}\right)^n J_n(s|z|) s ds,$$

with the coefficients of the decomposition given by the *Euclidean Fourier transform*

$$\widehat{f}(n, s) = \frac{i}{2} \int_{\mathbb{C}} f(z) \left(\frac{z}{|z|}\right)^{-n} J_n(s|z|) dz d\bar{z},$$

where $J_n(sr)$ are defined by the *Bessel function of order n* ,

$$J_n(z) = \frac{1}{2\pi} \int_0^{2\pi} e^{iz \sin \phi - in\phi} d\phi.$$

4. Geometry of the Camera Model. A detailed discussion of the conformal (projective) camera was given in [43]. In section 2.1 of that reference, we carefully explained how the image projective transformations are generated in the camera model (Figure 1 in [43]), and in section 6 we discussed the “conformal lens optics” of the camera and demonstrated some topological effects, artificial from the point of view of the image perspective transformations.

4.1. The Projective Camera. The camera has the pinhole located at the origin and the image plane consisting of points $(x_1, 1, x_3)$ identified with complex numbers $x_3 + ix_1$. Thus, the image of an object is obtained by projecting the object points into the image plane by

$$j(x_1, x_2, x_3) = \frac{x_3 + ix_1}{x_2}.$$

The camera is embedded into the complex plane

$$\mathbb{C}^2 = \left\{ \begin{pmatrix} z_1 \\ z_2 \end{pmatrix} \mid z_1 = x_2 + iy, z_2 = x_3 + ix_1 \right\}$$

such that the points of the image plane are the points where the complex lines $z_2 = \xi z_1$ intersect the line $z_1 = 1$. The action of the group $\mathbf{SL}(2, \mathbb{C})$ on nonzero column vectors in \mathbb{C}^2 induces the action on the “slopes” of lines $z_2 = \xi z_1$ by the following linear-fractional transformations:

$$(2) \quad \xi \mapsto \begin{pmatrix} a & b \\ c & d \end{pmatrix} \cdot \xi = \frac{d\xi + c}{b\xi + a}.$$

Therefore, the image plane can be regarded as the extended complex line $\widehat{\mathbb{C}} = \mathbb{C} \cup \{\infty\}$, where $j(x_1, 0, x_3) = \infty$.

We point out again that (2) transforms the slopes of the complex lines, that is, complex “directions,” which will be explained in the next section in terms of basic transformations: translations, dilations, and rotations. As the slopes $\xi = \xi_3 + i\xi_1$ are identified with the image plane points $x_3 + ix_1$ for $x_2 + iy = 1$, the transformation under $\mathbf{SL}(2, \mathbb{C})$ of complex lines in \mathbb{C}^2 induces projective transformations (2) of the points on the image plane. We note that the complex line $x_3 + ix_1 = (\xi_3 + i\xi_1)(x_2 + iy)$ with $y = 0$ corresponds to the line in \mathbb{R}^3 ,

$$\begin{pmatrix} x_1 \\ x_2 \\ x_3 \end{pmatrix} = \begin{pmatrix} \xi_1 \\ 1 \\ \xi_3 \end{pmatrix} t, \quad t \in \mathbb{R},$$

passing through the origin (*the ray passing through the pinhole*) and intersecting the image plane $x_2 = 1$ at the point $(\xi_1, 1, \xi_3)$.

4.2. Image Projective Transformations. The following subgroups of $\mathbf{SL}(2, \mathbb{C})$ acting on the image plane by (2) give all basic classes of the image projective transformations of *planar objects* or *patterns*:

(1) The maximal compact subgroup

$$(3) \quad \mathbf{SU}(2) = \left\{ \begin{pmatrix} \alpha & \beta \\ -\bar{\beta} & \bar{\alpha} \end{pmatrix} \mid |\alpha|^2 + |\beta|^2 = 1 \right\}$$

generates image projective transformations (with conformal distortions) by first rotating the projection in the camera of an image on $S^2_{(0,1,0)}$ and then projecting it back to the image plane. This follows from the fact that there is one-to-two correspondence between the group of rotations $\mathbf{SO}(3)$ and $\mathbf{SU}(2)$ —*the universal double covering group of $\mathbf{SO}(3)$* [8]. If the rotation $R(\psi, \phi, \psi') \in \mathbf{SO}(3)$ is parametrized by Euler angles, then α and β in (3) are given by

$$\alpha = \pm \cos(\phi/2) e^{i(\psi+\psi')/2}, \quad \beta = \pm i \sin(\phi/2) e^{i(\psi-\psi')/2};$$

see [8, 41]. Here the Euler angles are chosen such that ψ rotates about the x_2 -axis, followed by the rotation ϕ about the x'_3 -axis that is parallel to the x_3 -axis and passing through the sphere center $(0, 1, 0)$, and finally by the rotation ψ' about the rotated x_2 -axis. Thus the torus $\mathbf{M} = \left\{ \begin{pmatrix} e^{i\psi} & 0 \\ 0 & e^{-i\psi} \end{pmatrix} \right\} \subset \mathbf{SU}(2)$ describes rotations in the image plane.

(2) The subgroup

$$(4) \quad \mathbf{A} = \left\{ \begin{pmatrix} \rho & 0 \\ 0 & \rho^{-1} \end{pmatrix} \mid \rho > 0 \right\}$$

represents transformations (dilations by $1/\rho^2$) obtained by translating the image with respect to the optical axis of the camera and projecting it back to the image plane.

(3) Finally, the subgroup

$$(5) \quad \mathbf{N} = \left\{ \begin{pmatrix} 1 & 0 \\ \gamma & 1 \end{pmatrix} \mid \gamma \in \mathbb{C} \right\}$$

represents translations by γ in the image plane.

The group of image projective transformations is generated in the camera model by taking all finite iterations of the basic transformations induced by the groups

$\mathbf{SU}(2)$, \mathbf{A} , and $\overline{\mathbf{N}}$. It follows from the polar decomposition $\mathbf{SL}(2, \mathbb{C}) = \mathbf{SU}(2)\mathbf{ASU}(2)$ (see [27]) that this group is the group $\mathbf{SL}(2, \mathbb{C})$. This group is acting on the complex image plane by linear-fractional mappings (2).

The projective camera possesses the “conformal lens optics” because the linear-fractional transformations in (2) are conformal mappings; that is, they preserve angles; see [33]. Therefore, this camera is called the conformal camera. We refer to the procedure of correcting image projective transformations for conformal distortions as deconformalization of image projective transformations. We note that the conformal lens problem of the projective camera is similar to the problem of the absence of optical lenses in a pinhole camera; see the appendix in [31].

4.3. Geometry of the Image Plane. Geometry of the image plane $\widehat{\mathbb{C}}$, homogeneous under the action of $\mathbf{SL}(2, \mathbb{C})/\{\pm I\}$ by linear-fractional transformations, can be dually described as follows:

- (1) $\widehat{\mathbb{C}}$ is the complex projective line, i.e., $\widehat{\mathbb{C}} \cong P^1(\mathbb{C})$, where

$$P^1(\mathbb{C}) = \{\text{complex lines in } \mathbb{C}^2 \text{ through the origin}\}$$

with the group of projective transformations $\mathbf{PSL}(2, \mathbb{C}) = \mathbf{SL}(2, \mathbb{C})/\{\pm I\}$. Thus, the image projective transformations acting on the points of the image plane of the conformal camera can be identified with *projective geometry* of the one-dimensional complex line [9].

(2) $\widehat{\mathbb{C}}$ is the Riemann sphere since under stereographic projection $\sigma = j|_{S^2_{(0,1,0)}}$ we have the isomorphism $\widehat{\mathbb{C}} \cong S^2_{(0,1,0)}$. The group $\mathbf{PSL}(2, \mathbb{C})$ acting on $\widehat{\mathbb{C}}$ consists of the bijective meromorphic mappings of $\widehat{\mathbb{C}}$ [26], that is, the group of automorphisms of the Riemann sphere that preserve the intrinsic geometry imposed by complex structure, known as *Möbius geometry* [22] or *inversive geometry* [7].

4.4. The Relation of the Conformal Camera to Other Camera Models. The commonly used camera models in machine vision can be classified into calibrated and uncalibrated, with the different types of cameras in each category. The projective camera is the most general camera. It projects the points of space on an image plane. This projection can be written as a 3×4 real matrix in the corresponding homogeneous coordinates in space and in the image plane. Since scale is arbitrary for homogeneous coordinates and the mapping places no restrictions on the coordinates, it is called an uncalibrated camera. The other less general uncalibrated camera is the affine camera. It is a projective camera with the center of projection on the plane at infinity, which means that all projecting rays are parallel. The camera results in the composed effect of affine transformation between the space coordinates and the camera coordinates, parallel projection onto the image plane, and affine transformations of the image plane coordinates, given by the corresponding 3×4 real matrices.

Calibrated cameras are obtained by specifying camera parameters such as the focal length (the distance of the pinhole from the image plane) or the principal point, the point on the image plane at which the optical axis intersects the image plane. The most general calibrated camera is the perspective camera. This model uses central, that is, perspective, projections, reducing description to a pinhole camera with the optical axis perpendicular to the image plane and with coordinate systems related by Euclidean transformations. It again involves the corresponding 3×4 real matrices. Further restrictions result in less general cameras such as the weak perspective (the depth variation of objects along the viewing line is small compared with the viewing

distance) or the orthographic camera (orthographic projections). The classification of cameras with the corresponding matrices is given in [39].

The set of 3×4 matrices describing a particular camera does not form a group, which is a major obstacle in developing a group-theoretical approach to image representation that is well adapted to the image transformations produced by the camera. On the other hand, the conformal camera is characterized by the image projective transformations given by the action of the group $\mathbf{SL}(2, \mathbb{C})$ on the points of the image plane. Further, the group $\mathbf{SL}(2, \mathbb{C})$ has a well-understood Fourier analysis on it, which can provide the sophisticated framework of computational harmonic analysis to develop a data model for image representation well adapted to the projective image transformations. Thus, as the cameras are used in computer vision research to extract geometric information (for example, projective invariants) from scenes, the conformal camera is mainly used to construct an efficient computational framework for projectively covariant image representation. Another way of expressing it is to say that the cameras used in computer vision research belong to the geometric approach to image representation and rendering, while the conformal camera belongs to the imaging approach (see section 1).

Although the conformal camera is central to the development of the projective Fourier analysis later in the article, it is somewhat less intuitive than a pinhole camera commonly used in machine vision research. It could be the result of the way some of the projective deformations are generated by projecting an image from the image plane into the sphere, rotating the sphere, and then projecting the image back to the image plane. A quick look at the biological visual system should be useful in understanding that vision is too complicated a process for a pinhole camera to support. If we closely examine the human visual system, we realize that the retina of the eye (the camera with almost spherical image surface) does not “see”; rather, it contains photoreceptors (rod and cone cells) with chemicals that release energy when struck by light. The nervous system sends the retinal image (variations in released energy) to the primary visual cortex, an area in the visual cortex at the back of the brain. The brain processes visual information by sending it to many different visual areas (the exact function of which is not yet understood) and “sees” the image [25]. Certainly, the result of the human visual system is experimental evidence for an eye-centered spherical representation of the transformation from visual to motor coordinates [47].

5. The Group $\mathbf{SL}(2, \mathbb{C})$. Before we construct geometric Fourier analysis of the conformal camera, we need some analytical results for the group $\mathbf{SL}(2, \mathbb{C})$.

5.1. Gauss Decomposition. For each element $g = \begin{pmatrix} \alpha & \beta \\ \gamma & \delta \end{pmatrix} \in \mathbf{SL}(2, \mathbb{C})$, we have one of the two cases: $\alpha \neq 0$ or $\alpha = 0$.

(1) If $\alpha \neq 0$, then we can write

$$\begin{aligned} g &= \begin{pmatrix} 1 & 0 \\ \gamma/\alpha & 1 \end{pmatrix} \begin{pmatrix} \alpha & \beta \\ 0 & \alpha^{-1} \end{pmatrix} \\ &= \begin{pmatrix} 1 & 0 \\ \gamma/\alpha & 1 \end{pmatrix} \begin{pmatrix} \frac{\alpha}{|\alpha|} & 0 \\ 0 & \left(\frac{\alpha}{|\alpha|}\right)^{-1} \end{pmatrix} \begin{pmatrix} |\alpha| & 0 \\ 0 & |\alpha|^{-1} \end{pmatrix} \begin{pmatrix} 1 & \beta/\alpha \\ 0 & 1 \end{pmatrix}, \end{aligned}$$

where we used $\alpha\delta - \beta\gamma = 1$.

(2) If $\alpha = 0$, then

$$g = \begin{pmatrix} 0 & 1 \\ -1 & 0 \end{pmatrix} \begin{pmatrix} \beta^{-1} & -\delta \\ 0 & \beta \end{pmatrix}.$$

We conclude that for any $g \in \mathbf{SL}(2, \mathbb{C})$ either $g \in \overline{\mathbf{N}}\mathbf{B}$ or $g \in p\mathbf{B}$, where $\mathbf{B} = \mathbf{MAN}$ is the Bore subgroup and $p = \begin{pmatrix} 0 & 1 \\ -1 & 0 \end{pmatrix}$. Thus, we have the decomposition

$$(6) \quad \mathbf{SL}(2, \mathbb{C}) = \overline{\mathbf{N}}\mathbf{B} \cup p\mathbf{B},$$

which implies *Gauss decomposition*

$$(7) \quad \mathbf{SL}(2, \mathbb{C}) \doteq \overline{\mathbf{N}}\mathbf{MAN},$$

where “ \doteq ” means that equality holds except in a lower-dimensional subset $p\mathbf{B}$ of the invariant measure 0, that is, almost everywhere on $\mathbf{SL}(2, \mathbb{C})$. Furthermore, the map

$$\overline{\mathbf{N}} \times \mathbf{M} \times \mathbf{A} \times \mathbf{N} \rightarrow \mathbf{SL}(2, \mathbb{C}), \quad (\bar{n}, m, a, n) \mapsto \bar{n}man$$

is a diffeomorphism. If g factors under $\mathbf{SL}(2, \mathbb{C}) \doteq \overline{\mathbf{N}}\mathbf{MAN}$, then $g = \bar{n}(g)m(g)a(g)n$.

5.2. Iwasawa Decomposition. For a given $g = \begin{pmatrix} \alpha & \beta \\ \gamma & \delta \end{pmatrix} \in \mathbf{SL}(2, \mathbb{C})$ we want to write $g = kan$ with $k \in \mathbf{SU}(2)$, $a \in \mathbf{A}$, and $n \in \mathbf{N}$. In explicit terms this decomposition is given as follows:

$$g = \begin{pmatrix} \frac{\alpha}{\sqrt{|\alpha|^2 + |\gamma|^2}} & \frac{-\bar{\gamma}}{\sqrt{|\alpha|^2 + |\gamma|^2}} \\ \frac{\gamma}{\sqrt{|\alpha|^2 + |\gamma|^2}} & \frac{\bar{\alpha}}{\sqrt{|\alpha|^2 + |\gamma|^2}} \end{pmatrix} \begin{pmatrix} \sqrt{|\alpha|^2 + |\gamma|^2} & 0 \\ 0 & 1/\sqrt{|\alpha|^2 + |\gamma|^2} \end{pmatrix} \begin{pmatrix} 1 & \frac{\bar{\alpha}\beta + \bar{\gamma}\delta}{|\alpha|^2 + |\gamma|^2} \\ 0 & 1 \end{pmatrix},$$

which also shows its uniqueness. Further, we see from the above decomposition that the multiplication map

$$\mathbf{SU}(2) \times \mathbf{A} \times \mathbf{N} \rightarrow \mathbf{SL}(2, \mathbb{C}), \quad (k, a, n) \mapsto kan$$

is a diffeomorphism onto.

The decomposition

$$(8) \quad \mathbf{SL}(2, \mathbb{C}) = \mathbf{SU}(2)\mathbf{A}\mathbf{N}$$

is called the *Iwasawa decomposition* of $\mathbf{SL}(2, \mathbb{C})$. If $g \in \mathbf{SL}(2, \mathbb{C})$ decomposes under $\mathbf{SU}(2)\mathbf{A}\mathbf{N}$, we write $g = k(g)a'(g)n$.

5.3. Integral Formulas. The group $\mathbf{SL}(2, \mathbb{C})$ is unimodular and its invariant measure is the following: if $g = \begin{pmatrix} \alpha & \beta \\ \gamma & \delta \end{pmatrix} \in \mathbf{SL}(2, \mathbb{C})$, then $dg = (1/|\delta|^2)d\beta d\bar{\beta}d\gamma d\bar{\gamma}d\delta d\bar{\delta}$. Recall that if $\beta = \beta_1 + i\beta_2$, then $(i/2)d\beta d\bar{\beta} = d\beta_1 d\beta_2$. This is not defined on the set of measure 0 where $\delta = 0$. The Borel subgroup $\mathbf{B} \subset \mathbf{SL}(2, \mathbb{C})$ is not unimodular. In fact, if $b = \begin{pmatrix} \alpha & \beta \\ 0 & \alpha^{-1} \end{pmatrix} \in \mathbf{B}$, a left-invariant measure on \mathbf{B} is $d_l b = (i/2)^2(1/|\alpha|^4)d\alpha d\bar{\alpha}d\beta d\bar{\beta}$ and a right-invariant measure is given by $d_r b = |\alpha|^4 d_l b$. Thus the modular function on \mathbf{B} is $\Delta_{\mathbf{B}}(\begin{pmatrix} \alpha & \beta \\ 0 & \alpha^{-1} \end{pmatrix}) = |\alpha|^4$.

The decompositions of $\mathbf{SL}(2, \mathbb{C})$ discussed above lead to three important formulas that relate some invariant measures. They are corollaries of the following more general results from geometric analysis [27].

THEOREM 4. *Let \mathbf{G} be a unimodular Lie group and \mathbf{S} and \mathbf{P} be closed subgroups such that $\mathbf{S} \cap \mathbf{P}$ is compact and the set of products \mathbf{SP} exhausts \mathbf{G} except possibly for a set of invariant measure 0, that is, $\mathbf{G} \doteq \mathbf{SP}$. Then the left-invariant measures $d_l s$ and $d_l p$ on \mathbf{S} and \mathbf{P} , respectively, can be normalized so that*

$$\int_{\mathbf{G}} f(g)dg = \int_{\mathbf{S} \times \mathbf{P}} f(sp)\Delta_{\mathbf{P}}(p)d_l s d_l p = \int_{\mathbf{S} \times \mathbf{P}} f(sp)d_l s d_r p.$$

- COROLLARY 5. (1) If $\mathbf{SL}(2, \mathbb{C}) = \mathbf{SU}(2)\mathbf{AN}$, then $dg = dk d_r(an)$.
 (2) If $\mathbf{SL}(2, \mathbb{C}) = \mathbf{SU}(2)\mathbf{MAN}$, then $dg = dk d_r(man)$.
 (3) If $\mathbf{SL}(2, \mathbb{C}) \doteq \bar{\mathbf{N}}\mathbf{MAN}$, then $dg = d\bar{n} d_r(man)$.

REMARK 6. It follows from Iwasawa decomposition that $\mathbf{SL}(2, \mathbb{C})/\mathbf{B} = \mathbf{SU}(2)/\mathbf{M}$, and hence, isomorphic to both S^2 and $P^1(\mathbb{C})$. Since $\mathbf{SL}(2, \mathbb{C})$ is unimodular and \mathbf{B} is not, the invariant measure on $\mathbf{SL}(2, \mathbb{C})/\mathbf{B} \cong P^1(\mathbb{C}) \cong \hat{\mathbb{C}}$ does not exist. However, the Lebesgue measure $d\mu(z) = \frac{i}{2} dz d\bar{z}$ on $\hat{\mathbb{C}}$ is quasi-invariant and $d\mu(g^{-1} \cdot z) = |-bz + d|^{-4} d\mu(z)$, where $g = \begin{pmatrix} \alpha & \beta \\ \gamma & \delta \end{pmatrix} \in \mathbf{SL}(2, \mathbb{C})$. Thus, the unitary representation (1) on the homogeneous space $\mathbf{SL}(2, \mathbb{C})/\mathbf{B}$ involves the factor

$$\sqrt{\frac{d\mu(g^{-1} \cdot z)}{d\mu(z)}} = |-\beta z + \delta|^{-2},$$

which will appear in the principal series representations of $\mathbf{SL}(2, \mathbb{C})$.

6. Inducing Representations of the Principal Series of $\mathbf{SL}(2, \mathbb{C})$. Every representation \mathcal{T} of a Lie group \mathbf{G} on a Hilbert space H defines a representation of a closed subgroup $\mathbf{H} \subset \mathbf{G}$ on H by restricting \mathcal{T} to \mathbf{H} . Inducing representations is inverse to restricting; a representation of a Lie group \mathbf{G} is constructed from a representation of a subgroup \mathbf{H} . For many important Lie groups, inducing representations is a fundamental method of obtaining all irreducible unitary representations of \mathbf{G} that supply the building blocks of Fourier analysis on \mathbf{G} or its homogeneous spaces.

To describe the method of inducing representations, we let \mathbf{K} be a closed subgroup of a Lie group \mathbf{G} , both assumed to be unimodular with the invariant measures dk and dg , respectively. Further, assume that $\mathbf{G} = \mathbf{KP}$ with a closed subgroup \mathbf{P} , such that the map $(k, p) \mapsto kp$ of $\mathbf{K} \times \mathbf{P} \rightarrow \mathbf{G}$ is a bijection. Then $\mathbf{G}/\mathbf{P} \cong \mathbf{K}$ is a homogeneous space on which \mathbf{G} operates on the left.

Let Π be a representation of \mathbf{P} on a Hilbert space H . Further, let H^Π be the space of continuous mappings $F : \mathbf{G} \rightarrow H$ satisfying the condition $F(gp) = \Delta_{\mathbf{P}}(p)^{-1/2} \Pi(p)^{-1} F(g)$, where $\Delta_{\mathbf{P}}$ is the modular function on \mathbf{P} . The decomposition $\mathbf{G} = \mathbf{KP}$ shows that F is determined by its restriction to \mathbf{K} and we can define the norm of F by

$$(9) \quad \|F\|^2 = \int_{\mathbf{K}} |F(k)|^2 dk.$$

Then the representation \mathcal{U}^Π of \mathbf{G} on H^Π is given by the left action $\mathcal{U}^\Pi(g)F(x) = F(g^{-1}x)$. The actual representation \mathcal{U}^Π and the Hilbert space is obtained by completion in the norm (9). \mathcal{U}^Π is called the *induced representation* of Π to \mathbf{G} . The basic result is the following: if the representation Π is unitary, then the induced representation \mathcal{U}^Π is unitary.

The group $\mathbf{SL}(2, \mathbb{C})$ admits the Iwasawa decomposition $\mathbf{SL}(2, \mathbb{C}) = \mathbf{SU}(2)\mathbf{B}$, where the Borel subgroup \mathbf{B} has the form $\mathbf{B} = \mathbf{MAN}$, where \mathbf{N} is normal in \mathbf{B} . The unitary representations of $\mathbf{SL}(2, \mathbb{C})$, all of which are infinite-dimensional, are induced from the one-dimensional unitary representations of \mathbf{B} .

To this end, we first describe all finite irreducible unitary representations of \mathbf{B} . Let Π be any irreducible unitary representation of \mathbf{MA} on the Hilbert space \mathbb{C} . Since \mathbf{N} is normal in \mathbf{B} , we can extend Π to \mathbf{B} by $\Pi(dn) = \Pi(d)$, $d \in \mathbf{MA}$, $n \in \mathbf{N}$. See [24] for an explicit demonstration of this fact. Let $b = \begin{pmatrix} \alpha & \beta \\ 0 & \alpha^{-1} \end{pmatrix} \in \mathbf{B}$; then the unitary

representation $\Pi_{s,k}(b)$, $k \in \mathbb{Z}$, $s \in \mathbb{R}$, acts on \mathbb{C} by

$$\Pi_{s,k}(b)z = |\alpha|^{is} \left(\frac{\alpha}{|\alpha|} \right)^k z.$$

These one-dimensional unitary representations are all of the finite irreducible unitary representations of the Borel subgroup \mathbf{B} ; see [35]. Finally, recalling that the modular function on \mathbf{B} is $\Delta_{\mathbf{B}}(b) = |\alpha|^4$, we conclude that the space H^Π of the induced representations is given by

$$(10) \quad H^\Pi = \left\{ F \in C(\mathbf{SL}(2, \mathbb{C})) \mid F(gman) = |\alpha|^{-is-2} \left(\frac{\alpha}{|\alpha|} \right)^{-l} F(g) \right\}$$

with the norm

$$(11) \quad \|F\|^2 = \int_{\mathbf{SU}(2)} |F(k)|^2 dk.$$

The induced unitary representation of $\mathbf{SL}(2, \mathbb{C})$ is then obtained from $\mathcal{T}^\Pi(g)F(x) = F(g^{-1}x)$ by completing it in the norm (11).

It follows from the Gauss decomposition $\mathbf{SL}(2, \mathbb{C}) \doteq \overline{\mathbf{N}}\mathbf{B}$ that the restriction of $(\mathcal{T}^\Pi(g), H^\Pi)$ to $\overline{\mathbf{N}} \cong \mathbb{C}$ is one-to-one. Under this restriction, the resulting dense subspace is

$$(12) \quad H^\Pi = \left\{ F \in C(\overline{\mathbf{N}}) \mid F(\overline{n}man) = |\alpha|^{-is-2} \left(\frac{\alpha}{|\alpha|} \right)^{-l} F(\overline{n}) \right\}$$

and the action of the representation, called the *principal series* of $\mathbf{SL}(2, \mathbb{C})$, is obtained, using calculations done for the Gauss decomposition, as follows:

$$(13) \quad \begin{aligned} \mathcal{T}^\Pi(g)F(\overline{n}) &= F(g^{-1}\overline{n}) \\ &= F(\overline{n}(g^{-1}\overline{n})m(g^{-1}\overline{n})a(g^{-1}\overline{n})n) \\ &= |-\beta z + \delta|^{-is-2} \left(\frac{-\beta z + \delta}{|-\beta z + \delta|} \right)^{-k} F\left(\begin{pmatrix} 1 & 0 \\ \frac{\alpha z - \gamma}{-\beta z + \delta} & 1 \end{pmatrix} \right), \end{aligned}$$

where the norms of $L^2(\mathbf{SU}(2), dk)$ and $L^2(\overline{\mathbf{N}}, d\overline{n})$ are preserved under the restriction; that is,

$$\int_{\mathbf{SU}(2)} |F(k)|^2 dk = \int_{\overline{\mathbf{N}}} |F(\overline{n})|^2 d\overline{n}.$$

This restriction of the induced representations is called in representation theory the *noncompact picture* of induced representation and is particularly useful for studying the induced representations by analytic methods [27].

7. Geometric Fourier Analysis for Patterns. Projective Fourier analysis for patterns is constructed using the noncompact picture of induced representation. We start by noticing that for each $F \in H^\Pi$,

$$F(gman) = |\alpha|^{-is-2} \left(\frac{\alpha}{|\alpha|} \right)^{-l} F(g).$$

Therefore, $F(g)$ must be \mathbf{N} -invariant, and consequently, it can be written as a function on $\mathbb{C}^2 \setminus \{0\}$ (also denoted by F):

$$F\left(\begin{pmatrix} z_1 \\ z_2 \end{pmatrix}\right) = F\left(\begin{pmatrix} z_1 & \beta \\ z_2 & \delta \end{pmatrix} \begin{pmatrix} 1 \\ 0 \end{pmatrix}\right), \quad g = \begin{pmatrix} z_1 & \beta \\ z_2 & \delta \end{pmatrix} \in \mathbf{SL}(2, \mathbb{C}).$$

(In the group-theoretic formalism (see section 2), the group \mathbf{N} is the isotropy group of $\begin{pmatrix} 1 \\ 0 \end{pmatrix} \in \mathbb{C}^2 \setminus \{0\}$, implying that $\mathbb{C}^2 \setminus \{0\}$ is isomorphic to the homogeneous space \mathbf{G}/\mathbf{N} .) We verify that $F \in H^{\Pi(s,k)}$ if and only if

$$F\left(\begin{pmatrix} \lambda z_1 \\ \lambda z_2 \end{pmatrix}\right) = \lambda^m \bar{\lambda}^n F\left(\begin{pmatrix} z_1 \\ z_2 \end{pmatrix}\right) = |\lambda|^{is-2} \left(\frac{\lambda}{|\lambda|}\right)^k F\left(\begin{pmatrix} z_1 \\ z_2 \end{pmatrix}\right),$$

where $m = (1/2)(k + is) - 1$ and $n = (1/2)(-k + is) - 1$. Moreover,

$$F\left(\begin{pmatrix} z_1 \\ z_2 \end{pmatrix}\right) = |z_1|^{is-2} \left(\frac{z_1}{|z_1|}\right)^k F\left(\begin{pmatrix} 1 \\ \frac{z_2}{z_1} \end{pmatrix}\right) = |z_1|^{is-2} \left(\frac{z_1}{|z_1|}\right)^k \Phi\left(\frac{z_2}{z_1}\right),$$

where $\Phi(z) = F\left(\begin{pmatrix} 1 \\ z \end{pmatrix}\right)$. At this point we are dealing with homogeneous functions F on $\mathbb{C}^2 \setminus \{0\}$, the space of functions on which the irreducible representations of $\mathbf{SL}(2, \mathbb{C})$ were originally constructed in [15]. We note that from (13) it follows that

$$\mathcal{T}^{\Pi(s,k)} \Phi(z) = |-\beta z + \delta|^{-is-2} \left(\frac{-\beta z + \delta}{|-\beta z + \delta|}\right)^{-k} \Phi\left(\frac{\alpha z - \gamma}{-\beta z + \delta}\right),$$

which extends to the principal series representation of $\mathbf{SL}(2, \mathbb{C})$ on $L^2(\mathbb{C})$ [15, 27]. See Remark 6 in section 5.3 for the origin of the factor $|-\beta z + \delta|^{-2}$ present in the principal series representation.

For a given pattern's intensity function $f(z)$ we place it on the image plane $z_1 = 1$ of the conformal camera by writing $h\left(\begin{pmatrix} 1 \\ z \end{pmatrix}\right) \equiv f(z)$, and we extend to \mathbb{C}^2 along the complex lines as follows: $h\left(\begin{pmatrix} \xi \\ \xi z \end{pmatrix}\right) = |\xi|^{-1} f(\xi z)$. First we note that the action of $\mathbf{SL}(2, \mathbb{C})$ on h given by $h(g^{-1}\begin{pmatrix} z_1 \\ z_2 \end{pmatrix})$ induces the projective transformation $f(g^{-1} \cdot z)$ of the pattern f [41]. Then we define functions

$$F\left(\begin{pmatrix} z_1 \\ z_2 \end{pmatrix}\right) = \frac{i}{2} \int h\left(\begin{pmatrix} \mu z_1 \\ \mu z_2 \end{pmatrix}\right) |\mu|^{-is} \left(\frac{\mu}{|\mu|}\right)^{-k} d\mu d\bar{\mu}$$

and verify that F is in the representation space H^{Π} . We denote the restriction of this F to the image plane by $\Phi(z; k, s)$ and express it in terms of the pattern's intensity function $f(z)$,

$$\Phi(z; k, s) = \frac{i}{2} \int f(\mu z) |\mu|^{-is-1} \left(\frac{\mu}{|\mu|}\right)^{-k} d\mu d\bar{\mu}.$$

Changing variable $\xi = \mu z$ yields $\Phi(z; k, s) = |z|^{is-1} \left(\frac{z}{|z|}\right)^k \widehat{f}(s, k)$, where

$$(14) \quad \widehat{f}(s, k) = \frac{i}{2} \int f(\xi) |\xi|^{-is-1} \left(\frac{\xi}{|\xi|}\right)^{-k} d\xi d\bar{\xi}$$

is the *projective Fourier transform* (PFT) of the pattern f . In log-polar coordinates (u, θ) given by $\xi = e^{u+i\theta}$, $\widehat{f}(k, s)$ has the form of the standard Fourier integral, given

in the next section by (16). Inverting it (see [41]), we get the *inverse projective Fourier transform*

$$(15) \quad f(z) = \frac{1}{(2\pi)^2} \sum_{k=-\infty}^{\infty} \int \widehat{f}(s, k) |z|^{is-1} \left(\frac{z}{|z|}\right)^k ds.$$

Also, the usual Plancherel’s theorem gives the following projective counterpart of it:

$$\frac{i}{2} \int |f(z)|^2 dz d\bar{z} = \frac{1}{(2\pi)^2} \sum_{k=-\infty}^{\infty} \int |\widehat{f}(s, k)|^2 ds.$$

We see that the inverse projective Fourier transform provides decomposition in terms of the characters $|z|^{is} \left(\frac{z}{|z|}\right)^k$ of the Borel subgroup $\mathbf{B} \subset \mathbf{SL}(2, \mathbb{C})$ with the coefficients given by the projective Fourier transform. We note that the Gauss decomposition $\mathbf{SL}(2, \mathbb{C}) \doteq \bar{\mathbf{N}}\mathbf{B}$ implies that \mathbf{B} exhausts the “projective” part of $\mathbf{SL}(2, \mathbb{C})$ as $\bar{\mathbf{N}} \cong \mathbb{C}$ represents translations in the image plane. It should be seen in light of the fact that all unitary representations of the group $\mathbf{SL}(2, \mathbb{C})$ are infinite-dimensional [15], as opposed to the fact we have mentioned before that all finite-dimensional irreducible unitary representations of the Borel group \mathbf{B} are in fact one-dimensional.

8. The Discrete Projective Fourier Transform. In log-polar coordinates (u, θ) given by $z = e^u e^{i\theta}$, PFT in (14) has the standard Fourier integral form

$$(16) \quad \widehat{f}(s, k) = \int_0^{2\pi/L} \int_{\ln r_a}^{\ln r_b} g(u, \theta) e^{-i(us+\theta k)} du d\theta = \widetilde{g}(s, k),$$

where the support of $g(u, \theta) = e^u f(e^{u+i\theta})$ is assumed to be within $[\ln r_a, \ln r_b] \times [0, 2\pi/L]$ with $L \in \mathbb{N}$. Also, \widetilde{g} denotes here the standard Fourier transform of g . Hence, extending $g(u, \theta)$ periodically $g(u+mT, \theta+2\pi n/L) = g(u, \theta)$ where $T = \ln \frac{r_b}{r_a}$, it can be expanded in a double Fourier series [42],

$$(17) \quad g(u, \theta) = \frac{L}{2\pi T} \sum_{m=-\infty}^{\infty} \sum_{n=-\infty}^{\infty} \widehat{f}\left(\frac{2\pi m}{T}, nL\right) e^{i(2\pi mu/T+nL\theta)},$$

where

$$(18) \quad \begin{aligned} \widetilde{g}\left(\frac{2\pi m}{T}, nL\right) &= \widehat{f}\left(\frac{2\pi m}{T}, nL\right) \\ &= \int_0^{2\pi/L} \int_{\ln r_a}^{\ln r_b} g(u, \theta) e^{-i(2\pi mu/T+nL\theta)} du d\theta. \end{aligned}$$

An efficient computation of the PFT \widehat{f} must involve only a finite number of algebraic operations performed on a finite set of data. To this end, assuming that

$$(19) \quad \text{supp } \widetilde{g} = \text{supp } \widehat{f} \subset [-\Omega, \Omega] \times [-\Gamma, \Gamma]$$

and approximating the integral in (18) by a double Riemann sum with $M \times N$ partition points $(u_k, \theta_l) = (\ln r_a + kT/M, 2\pi l/LN)$, $0 \leq k \leq M-1$, $0 \leq l \leq N-1$, we obtain

$$\widehat{f}\left(\frac{2\pi m}{T}, nL\right) \approx \frac{2\pi T}{LNM} \sum_{k=0}^{M-1} \sum_{l=0}^{N-1} g(u_k, \theta_l) e^{-2\pi i(mk/M+nl/N)},$$

where $|m| \leq \Omega T/2\pi$ and $|n| \leq \Gamma/L$.

For this procedure to yield a good approximation, the spacing of partition points $\delta_1 = T/M$ and $\delta_2 = 2\pi/LN$ must be quite small compared with the corresponding wave lengths of the exponentials in (18), namely, $T/|m|$ and $2\pi/|n|L$, respectively. Consequently, we must assume that $|m| \ll M$ and $|n| \ll N$, and choose $M \gg \Omega T/2\pi$, $N \gg \Gamma/L$.

In short, using the approximation procedure outlined above, one can arrive (see [23] for a discussion of the numerical aspects of the approximation) at the expressions

$$(20) \quad \widehat{f}_{m,n} = \sum_{k=0}^{M-1} \sum_{l=0}^{N-1} f_{k,l} e^{u_k} e^{-i2\pi nl/N} e^{-i2\pi mk/M}$$

and

$$(21) \quad f_{k,l} = \frac{1}{MN} \sum_{m=0}^{M-1} \sum_{n=0}^{N-1} \widehat{f}_{m,n} e^{-u_k} e^{i2\pi nl/N} e^{i2\pi mk/M},$$

where $f_{k,l} = (2\pi T/LMN)g(u_k, \theta_l)e^{-u_k}$ and $\widehat{f}_{m,n} = \widehat{f}\left(\frac{2\pi m}{T}, nL\right)$. We note that $\widehat{f}_{m,n}$ is (M, N) -periodic. Both expressions (20) and (21) can be computed efficiently by FFT algorithms.

On introducing $z_{k,l} = e^{u_k + i\theta_l}$ into (20) and (21), we obtain the (M, N) -point discrete projective Fourier transform (DPFT) and its inverse,

$$(22) \quad \widehat{f}_{m,n} = \sum_{k=0}^{M-1} \sum_{l=0}^{N-1} f_{k,l} \left(\frac{z_{k,l}}{|z_{k,l}|} \right)^{-nL} |z_{k,l}|^{-\frac{i2\pi m}{T} + 1}$$

and

$$(23) \quad f_{k,l} = \frac{1}{MN} \sum_{m=0}^{M-1} \sum_{n=0}^{N-1} \widehat{f}_{m,n} \left(\frac{z_{k,l}}{|z_{k,l}|} \right)^{nL} |z_{k,l}|^{\frac{i2\pi m}{T} - 1},$$

now with $f_{k,l} = (2\pi T/LMN)f(z_{k,l})$. Its projectively adapted characteristics are expressed as follows:

$$(24) \quad f'_{k,l} = \frac{1}{MN} \sum_{m=0}^{M-1} \sum_{n=0}^{N-1} \widehat{f}_{m,n} \left(\frac{z'_{k,l}}{|z'_{k,l}|} \right)^{nL} |z'_{k,l}|^{i2\pi m/T - 1},$$

where $z'_{k,l} = g^{-1} \cdot z_{k,l}$, $g \in \mathbf{SL}(2, \mathbb{C})$, and $f'_{k,l} = (2\pi T/LMN)f(z'_{k,l})$. We note that in (24) only the DPFT of the original (undistorted) pattern is involved.

9. DPFT in Digital Image Processing. The DPFT is implemented in the image processing environment provided by the MATLAB Image Processing Toolbox. To convert analog images to the digital form and compute their discrete Fourier transforms efficiently by applying the FFT algorithms, the toolbox supports the standard (uniform) sampling with rectangular pixel geometry. However, the DPFT has the standard Fourier integral form in log-polar coordinates. Therefore, we must resample an image such that the sampling geometry in the log-polar coordinate plane consists of equal rectangular pixels. This resampling procedure is referred to as the sampling interface.

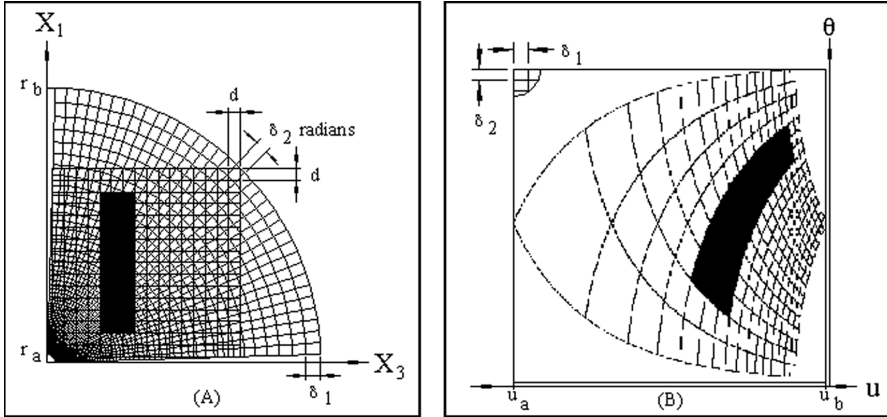


Fig. 1 Geometry of the sampling interface. (a) The log-polar (nonuniform) sampling of the bar pattern in the image plane. (b) The (uniform) sampling copy of the bar pattern in the log-plane coordinate plane.

9.1. The Sampling Interface. The sampling interface is explained in Figure 1.

The minimal rate of the log-polar sampling depends on the resolution of the image. We require for our calculations that the upper right pixel is covered by one sector of the log-polar partition whose area is approximately the area of the pixel; see Figure 1(a). Otherwise, the number of sectors per this pixel is a user-supplied parameter, if one needs to increase or decrease the image resolution.

If the digital image in the log-polar plane is represented by the corresponding $M \times N$ image matrix, it has a resolution of $M \times N$. To determine M and N , or equivalently δ_1 and δ_2 , we assume that the pattern size in the image plane is $A \times A$ and the pixel size is $d \times d$. Then a simple geometrical consideration gives (see Figure 1) the following relations between dimensions of pixels: $\delta_1 = -\ln(1 - d/r_b)$ and $\delta_2 = d/r_b$ radians, where $r_b - r_a = \sqrt{2}A$. Thus, in practice, $d \ll r_b$ and we can always take $\delta_1 = \delta_2 = \delta$, where $\delta = d / (r_a + \sqrt{2}A)$. Therefore, the resolution $M \times N$ of the image in log-polar coordinates is given by

$$M = \frac{r_a + \sqrt{2}A}{d} \ln \left(\frac{r_a + \sqrt{2}A}{r_a} \right), \quad N = \frac{\pi (r_a + \sqrt{2}A)}{2d},$$

where we have taken $L = 4$.

The bar pattern is shown in Figure 1(a) with $A = 16$, $r_a = 0.5$, and $d = 1$. Then, we obtain $\delta = 0.04$, $M = 89$, and $N = 35$. However, the bar pattern in Figure 1(b) has been rendered in the log-polar coordinate plane, using the sampling interface algorithm, with an increased resolution of 300×300 to smoothen pixel boundaries.

9.2. Band-Limited Images. Often one can assume that a given pattern has a bounded spectrum $[-\omega, \omega] \times [-\omega, \omega]$. The value of ω could be determined, for example, by the rate at which the Fourier transform of the pattern is decaying for large spatial frequencies. The *Nyquist condition* requires that the sampling distance d satisfies the relation $d = \pi/\omega$ in both the x - and y -axis directions. Recalling that in the log-polar plane $\delta = T/M = 2\pi/LN$, we have $M = \omega r_b T/\pi$ and $N = 2\omega r_b/L$, where $T = \ln \frac{r_b}{r_a}$. Thus, we can obtain the log-polar radial and angular frequencies Ω and

Γ (cf. (19)) corresponding to the spatial frequency ω using the Nyquist condition as follows: $\delta = \pi/\Omega = \pi/\Gamma$. Thus, we conclude that the radial and angular frequencies Ω and Γ satisfy the relation $\Omega = \Gamma = (r_a + \sqrt{2}A)\omega$.

9.3. Image Projective Transformations. How does one compute efficiently the projectively transformed pattern $f'_{m,n}$, represented in (24) in terms of $[\widehat{f}_{k,l}]$? We discuss this for elements of the group $\mathbf{SL}(2, \mathbb{C})$ given by

$$(25) \quad g = \begin{pmatrix} \cos \frac{\phi}{2} & i \sin \frac{\phi}{2} \\ i \sin \frac{\phi}{2} & \cos \frac{\phi}{2} \end{pmatrix} \in \mathbf{SU}(2),$$

which represent the rotations about the x'_3 -axis by the angle $-\phi$ of the pattern in the conformal camera model; see section 2. Then the action is given by

$$(26) \quad z'_{m,n} = g^{-1} \cdot z_{m,n} = \frac{z_{m,n} \cos \frac{\phi}{2} - i \sin \frac{\phi}{2}}{-iz_{m,n} \sin \frac{\phi}{2} + \cos \frac{\phi}{2}}.$$

Under this transformation, the equally spaced points (u_m, θ_n) transform into points $(u'_{m,n}, \theta'_{m,n})$ with the coordinates satisfying the equations

$$(27) \quad e^{2u'_{m,n}} = \frac{e^{2u_m} \cos^2 \frac{\phi}{2} + \sin^2 \frac{\phi}{2} - e^{u_m} \sin \phi \sin \theta_n}{e^{2u_m} \sin^2 \frac{\phi}{2} + \cos^2 \frac{\phi}{2} + e^{u_m} \sin \phi \sin \theta_n}$$

and

$$(28) \quad \tan \theta'_{m,n} = \frac{1/2(e^{2u_m} - 1) \sin \phi + e^{u_m} \sin \theta_n \cos \phi}{e^{u_m} \cos \theta_n}.$$

In terms of $(u'_{m,n}, \theta'_{m,n})$, (24) is now expressed by

$$(29) \quad f'_{m,n} = \frac{1}{MN} \sum_{k=0}^{M-1} \sum_{l=0}^{N-1} \widehat{f}_{k,l} e^{-u'_{m,n}} e^{i2\pi u'_{m,n} k/T} e^{i\theta'_{m,n} lL}.$$

We note that $f'_{m,n}$ denotes the value $f_{m,n}$ given in (24) but taken at $(u'_{m,n}, \theta'_{m,n})$ such that $z'_{m,n} = e^{u'_{m,n}} e^{i\theta'_{m,n}}$.

Now, the equally spaced property of the samples is destroyed. However, recent advances in nonuniform sampling theory [12, 34] allow the development of such efficient algorithms in log-polar coordinate space.

9.4. The Deconformalization Problem. As we have already mentioned (see [43] for detailed discussion), the image projective transformations in (29) need corrections for distortions due to the ‘‘conformal lens optics’’ of the projective camera model in order to display the image perspective transformations.

The correction for conformal distortions of the projective transformations of pixels is done as follows. We choose the ‘‘midpoint’’ $\eta = b + ia$ of the pattern and extend the projection of the pattern from the sphere $S^2_{(0,1,0)}$ to the plane T_p tangent to the sphere at the point

$$p = \sigma^{-1}(\eta) = \left(\frac{2a}{a^2 + b^2 + 1}, \frac{2}{a^2 + b^2 + 1}, \frac{2b}{a^2 + b^2 + 1} \right),$$

where $\sigma = j|_{S^2_{(0,1,0)}}$ is the stereographic projection. After rotating the sphere $S^2_{(0,1,0)}$ (with the tangent plane T_p attached to it) about the x'_3 -axis by the angle $-\phi$, as

given by (26), and projecting back from the (rotated) tangent plane, we obtain the projective transformations corrected for conformal distortions, that is, the perspective transformations. We refer to it as deconformalization of the image projective transformations.

The explicit calculations in this case give the following results. The real and imaginary parts of the coordinates $z'_{m,n} = x'_{3m,n} + ix'_{1m,n}$ of the projective transformations (26) are the following:

$$(30) \quad \begin{aligned} x'_{3m,n} &= \frac{2x_{3m,n}}{(x_{1m,n}^2 + x_{3m,n}^2)(1 - \cos \phi) + 2x_{1m,n} \sin \phi + \cos \phi + 1}, \\ x'_{1m,n} &= \frac{(x_{1m,n}^2 + x_{3m,n}^2) \sin \phi + 2x_{1m,n} \cos \phi - \sin \phi}{(x_{1m,n}^2 + x_{3m,n}^2)(1 - \cos \phi) + 2x_{1m,n} \sin \phi + \cos \phi + 1}. \end{aligned}$$

The transformed coordinates in (30) include conformal distortions. The corresponding coordinates $z''_{m,n} = x''_{3m,n} + ix''_{1m,n}$ of the projective transformation corrected for conformal distortions (with the chosen point $\eta = b + ia$) are given by

$$(31) \quad \begin{aligned} x''_{3m,n} &= \frac{2x_{3m,n}}{(2ax_{1m,n} - a^2 + 2bx_{3m,n} - b^2)(1 - \cos \phi) + 2x_{1m,n} \sin \phi + \cos \phi + 1}, \\ x''_{1m,n} &= \frac{(2ax_{1m,n} - a^2 + 2bx_{3m,n} - b^2) \sin \phi + 2x_{1m,n} \cos \phi - \sin \phi}{(2ax_{1m,n} - a^2 + 2bx_{3m,n} - b^2)(1 - \cos \phi) + 2x_{1m,n} \sin \phi + \cos \phi + 1}. \end{aligned}$$

The extension to general image projective transformations is simple and is not discussed further in this paper.

Finally, the coordinates (31) of the projectively transformed pixels can be used in a straightforward way to correct for conformal distortions of log-polar coordinates $(u'_{m,n}, \theta'_{m,n})$ given in (27) and (28). Those corrected log-polar coordinates are denoted by $(u''_{m,n}, \theta''_{m,n})$, in terms of which the *conformal-distortion free inverse DPFT* is given as follows:

$$(32) \quad f''_{m,n} = \frac{1}{MN} \sum_{k=0}^{M-1} \sum_{l=0}^{N-1} \hat{f}_{k,l} e^{-u''_{m,n}} e^{i2\pi u''_{m,n} k/T} e^{i\theta''_{m,n} lL}.$$

9.5. DPFT and Foveated Image Processing. The resampling procedure, referred to as the sampling interface, provides an example of foveated or space-variant image representation used for retina-like architecture of visual sensors of some cameras in active vision systems [3, 5, 36]. This architecture is based on variation of resolution across the visual field like that of the human visual system: the resolution decreases with the distance from the fovea, achieving variable data compression. It has been evidenced that the retinotopic mapping of the visual field to the visual cortex is characterized by a complex logarithmic transformation [37]. Since the principal complex logarithm,

$$\ln z = \ln r e^{i\theta} = \ln r + i\theta,$$

is identified with log-polar coordinates $(\ln r, \theta)$, it transforms the DPFT of a pattern with log-polar sampling (retinal image) into the standard discrete Fourier transform of the uniformly sampled pattern in the log-polar coordinate plane (cortical image).

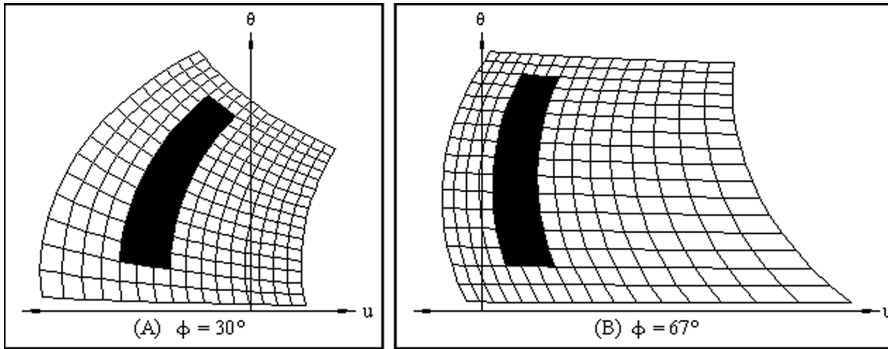


Fig. 2 Deconformalized image projective transformations of the bar pattern in the log-polar coordinate plane.

The framework of computational harmonic analysis can be used to efficiently process and analyze log-polar (cortical) patterns; see [46].

Despite the advantages (similarity invariance, compression), foveated sensors have not been widely used due to the lack of elegant image processing tools [48]. Because image processing based on DPFT naturally involves log-polar sampling geometry and is well adapted to image perspective transformations of planar objects, it should provide the right framework to develop the tools needed for active vision systems. For example, the presence of a planar surface of the moving object in a scene can be used to identify the object.

10. Computer Simulation for Binary Images. In this work we do not reconstruct patterns' image projective transformations based upon the expression (32), as it requires the implementation of nonuniform sampling. This implementation, important for gray-level images—as most natural images are, with 256 possible gray levels ranging from white to black—will be the subject of the next paper. Here we carry out the tests for binary digital patterns, in which image projective transformations are applied to the pixels' boundaries, avoiding the nonuniform sampling problem.

The sampling interface was implemented previously in MATLAB's Image Processing Toolbox by Ron Hoppe and it performed quite well [45]. In fact, the sampling interface algorithm was applied to the pattern of resolution 312×144 pixels and displayed it in the log-polar coordinate plane with resolution 2048×1024 pixels. This rather high resolution was needed there as the pattern contained a fine structure around the origin of the log-polar coordinates. Recall that the bar pattern in Figure 1(b) was displayed in the log-polar coordinate plane with a resolution of 300×300 pixels, by applying the sampling interface algorithm to the pattern in Figure 1(a).

Our numerical tests carried out for binary digital patterns include the deconformalization of image projective transformations of pixels, done in the log-polar coordinate plane (the step that for gray-level images will employ DPFT and nonuniform sampling), and then rendering them in the image plane by applying the sampling interface.

In Figure 2, the deconformalized image projective transformations of the bar pattern are displayed in the log-polar coordinate plane for the two indicated angles $-\phi$ in (25).

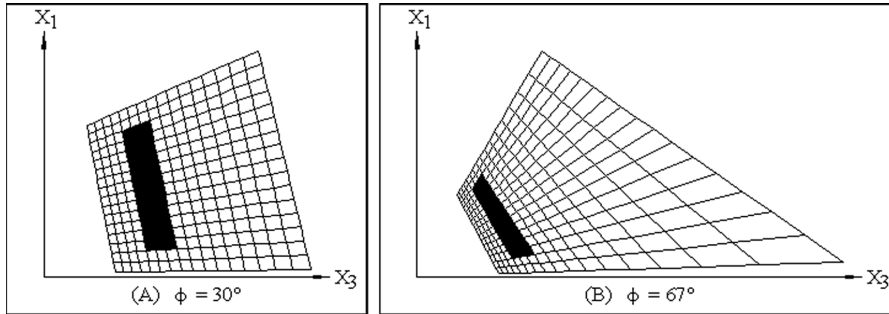


Fig. 3 Deconformalized image projective (perspective) transformations rendered in the image plane by using the sampling interface.

Next, the outputs from the sampling interface algorithm, applied to those two image projective transformations, are shown in Figure 3. We see in this figure the corresponding image perspective (deconformalized projective) transformations of the bar pattern in the image plane.

We stress that for gray-level images of natural patterns, we must work with projective Fourier representation of images (the inverse DPFT) in log-polar coordinates, since in this setting we can implement efficiently an algorithm reconstructing image projective transformations from nonuniform samples. Note that the nonuniform two-dimensional FFT is given in [12, 34], and the algorithm in [18] also contains it as one of the components.

II. Conclusions. In this article the framework of geometric Fourier analysis on groups and homogeneous spaces was discussed in the context of the projective-conformal camera, leading to the construction of projective Fourier analysis for patterns (i.e., planar objects). In this framework of harmonic analysis, the group $\mathbf{SL}(2, \mathbb{C})$ identified in the camera model acts by linear-fractional (conformal) mappings on the image plane homogeneous under the group action, providing image projective transformations. The inverse projective Fourier transform decomposes the intensity function of a pattern in terms of the unitary irreducible representations of the Borel subgroup of $\mathbf{SL}(2, \mathbb{C})$ with the coefficients of the decomposition given by the projective Fourier transform of the pattern. This decomposition encodes the projective covariance, as one can render patterns' projective (and perspective) transformations by computing only one projective Fourier transform of the original pattern. Its feasibility follows from these observations: (1) although all nontrivial unitary representations of the group $\mathbf{SL}(2, \mathbb{C})$ are infinite-dimensional, all finite unitary representations of the Borel subgroup are one-dimensional; (2) the Borel subgroup exhausts the “projective” part of $\mathbf{SL}(2, \mathbb{C})$.

Further, the data model for digital image representation based on the DPFT was developed and its projective covariance emphasized analytically and in the computer simulation of synthetic images. The DPFT has the form of the standard Fourier transform in log-polar coordinates. Thus, to convert analog patterns to the digital form by DPFT and to compute them by FFT, the *sampling interface*, exchanging uniform samplings of rectangular pixels between the image plane and the rectangular log-polar coordinate plane, was constructed. In particular, how the Nyquist sampling condition is effected by the interface was discussed. The projectively adapted property

(covariance) of the projective Fourier representation of a pattern allows one to render its image projective transformations by computing only DPFT of the original pattern. However, the correction for the *conformal lens optics* of the camera, the so-called *deconformalization* of image projective transformations, is needed to render image perspective transformations.

The log-polar sampling geometry, needed for efficient implementation of DPFT in digital image representation, is an example of foveated or space-variant image representation used in the active vision systems motivated by the human visual system. Given that there has been little systematic development of computational vision algorithms that are explicitly designed for foveated image representation, the computational framework of projective harmonic analysis presented in this article should set the stage for the development of elegant image processing and analysis tools for foveated vision.

Finally, it has been emphasized that nonuniform FFT should be used to render efficiently image projective transformations of natural digital patterns, as they involve 256 gray levels for a pixel. It has not been done in this work but it will be implemented in the future. It seems that the most computationally intensive component of the implementation is the sampling interface image plane and the log-polar plane. Since nonuniform sampling theory and practice are presently well understood [12, 18, 34], we do not expect to have difficulties with the implementation of an algorithm reconstructing images from nonuniform samples.

Acknowledgment. We thank Joe Flaherty for his editorial help and the anonymous referees for helpful comments.

REFERENCES

- [1] J.-P. ANTOINE, R. MURENZI, AND P. VANDERGHEYNST, *Two-dimensional directional wavelets in image processing*, Int. J. Imaging Systems and Technol., 7 (1996), pp. 152–165.
- [2] E.B. BARRETT, P.M. PAYTON, M.H. BRILL, AND N.N. HAAG, *Invariants under image perspective transformations: Theory and examples*, Int. J. Imaging Systems and Technol., 2 (1990), pp. 296–314.
- [3] E.B. BEDERSON, R.S. WALLECE, AND E.L. SCHWARTZ, *A miniaturized space-variant active vision system: Cortex-1*, Machine Vision Appl., 8 (1995), pp. 101–109.
- [4] N. BLATT AND J. RUBINSTEIN, *The Canonical coordinates method for pattern recognition. II. Isomorphism with affine transformations*, Pattern Recognition, 27 (1994), pp. 99–107.
- [5] J.A. BOLUDA, F. PARDO, T. KAYSER, J.J. PÉREZ, AND J. PELECHANO, *A new foveated space-variant camera for robotic applications*, in Proceedings of the IEEE Conference on Electronics, Circuits and Systems, Rhodes, Greece, 1996.
- [6] R. BRACEWELL, *The Fourier Transform and Its Applications*, 2nd ed., McGraw-Hill, New York, 1986.
- [7] D.A. BRANNAN, M.F. ESPLÉN, AND J.J. GRAY, *Geometry*, Cambridge University Press, Cambridge, UK, 1998.
- [8] Y. CHOQUET-BRUHAT AND C. DEWITT-MORETTE, *Analysis, Manifolds and Physics*, 2nd ed., North-Holland, Amsterdam, 1977.
- [9] D. COX, J. LITTLE, AND D. O’SHEA, *Ideals, Varieties, and Algorithms. An Introduction to Computational Algebraic Geometry and Commutative Algebra*, Springer-Verlag, New York, 1992.
- [10] D.L. DONOHO AND M.R. DUNCAN, *Digital Curvelet Transform: Strategy, Implementation and Experiments*, Preprint, Stanford University, Stanford, CA, 1999.
- [11] J.R. DRISCOLL AND D.M. HEALY, *Computing Fourier transforms and convolutions on the 2-sphere*, Adv. in Appl. Math., 15 (1994), pp. 202–250.
- [12] A.J.W. DULJANDAM AND M.A. SCHONEWILLE, *Nonuniform fast Fourier transform*, Geophysics, 64 (1999), pp. 539–551.
- [13] H.G. FEICHTINGER AND T. STROHMER, EDs., *Gabor Analysis and Algorithms. Theory and Applications*, Birkhäuser, Boston, 1998.

- [14] J.-P. GAUTHIER, G. BORNARD, AND M. SILBERMANN, *Motions and pattern analysis: Harmonic analysis on groups and their homogeneous spaces*, IEEE Trans. Syst. Man Cybernet., 21 (1991), pp. 149–172.
- [15] I.M. GELFAND, M.I. GRAEV, AND N.YA. VILENKIN, *Generalized Functions. Vol. 5: Integral Geometry and Representation Theory*, Academic Press, New York, 1966.
- [16] F. GHORBEL, *A complete invariant description for gray-level images by the harmonic analysis approach*, Pattern Recognition Lett., 15 (1994), pp. 1043–1051.
- [17] F. GIULIANINI, M. FERRARO, AND T.M. CAELLI, *Transformational properties of integral transforms of images*, J. Opt. Soc. Amer. A, 9 (1992), pp. 494–496.
- [18] K. GRÖCHENIG AND T. STROHMER, *Numerical and theoretical aspects of nonuniform sampling of band-limited images*, in Nonuniform Sampling. Theory and Practice, F. Marvasti, ed., Kluwer/Plenum, New York, 2001, pp. 283–324.
- [19] K.I. GROSS, *On the evolution of noncommutative harmonic analysis*, Amer. Math. Monthly, 85 (1977), pp. 525–548.
- [20] S. HELGASON, *Functions on symmetric spaces*, in Harmonic Analysis on Homogeneous Spaces, C.C. Moore, ed., Proc. Sympos. Pure Math. 26, AMS, Providence, RI, 1973, pp. 101–146.
- [21] S. HELGASON, *Topics in Harmonic Analysis on Homogeneous Spaces*, Birkhäuser, Boston, 1981.
- [22] M. HENLE, *Modern Geometries. The Analytical Approach*, Prentice-Hall, Upper Saddle River, NJ, 1997.
- [23] P. HENRICI, *Applied and Computational Complex Analysis*, Vol. 3, Wiley, New York, 1986.
- [24] R.A. HERB, *An elementary introduction to Harish-Chandra's work*, in The Mathematical Legacy of Harish-Chandra—A Celebration of Representation Theory and Harmonic Analysis, R.S. Doran and V.S. Varadarajan, eds., Proc. Sympos. Pure Math. 68, AMS, Providence, RI, 2000, pp. 59–75.
- [25] D.E. HUBEL, *Eye, Brain, and Vision*, Scientific American Library, New York, 1988.
- [26] G. JONES AND D. SINGERMAN, *Complex Functions*, Cambridge University Press, Cambridge, UK, 1987.
- [27] A.W. KNAPP, *Representation Theory of Semisimple Groups: An Overview Based on Examples*, Princeton University Press, Princeton, NJ, 1986.
- [28] T.-H. LI, *Multiscale representation and analysis of spherical data by spherical wavelets*, SIAM J. Sci. Comput., 21 (1999), pp. 924–953.
- [29] S.G. MALLAT, *Multifrequency channel decomposition of images and wavelet models*, IEEE Trans. Acoust. Speech Signal Process., 37 (1989), pp. 2091–2110.
- [30] D. MUMFORD, *Mathematical theories of shape: Do they model perception?*, in Geometric Methods in Computer Vision, B.C. Vemuri, ed., SPIE 1570, Bellingham, WA, 1991, pp. 2–10.
- [31] J.L. MUNDY AND A. ZISSERMAN, EDS., *Geometric Invariance in Computer Vision*, MIT Press, Cambridge, MA, 1992.
- [32] J.L. MUNDY AND A. ZISSERMAN, EDS., *Application of Invariance in Computer Vision II*, Proceedings of the Second European-U.S. Workshop on Invariance, Ponta Delgada, Azores, 1993.
- [33] T. NEEDHAM, *Visual Complex Analysis*, Clarendon Press, Oxford, 1997.
- [34] D. POTTS, G. STEIDL, AND M. TASCHE, *Fast Fourier transform for nonequispaced data: A tutorial* in Modern Sampling Theory: Mathematics and Applications, J.J. Benedetto and P. Ferreira, eds., Birkhäuser, Boston, 2001, pp. 247–270.
- [35] P.J. SALLY, JR., *Harmonic analysis and group representations*, in Studies in Harmonic Analysis, J.M. Ash, ed., MAA Stud. Math. 13, Math. Assoc. Amer., Washington, D.C., 1976, pp. 224–256.
- [36] G. SANDINI, P. QUESTA, D. SCHEFFER, B. DIERICKX, AND A. MANNUCCI, *A retina-like CMOS sensor and its applications*, in Proceedings of the 1st IEEE SAM Workshop, Cambridge, MA, 2000.
- [37] E.L. SCHWARTZ, *Spatial mapping in primate sensory projection: Analytical structure and relevance to perception*, Biological Cybernet., 25 (1977), pp. 181–194.
- [38] J. SEGMAN, J. RUBINSTEIN, AND Y.Y. ZEEVI, *The canonical coordinates method for pattern recognition: Theoretical and computational considerations*, IEEE Trans. Pattern Anal. Mach. Intell., 14 (1992), pp. 1171–1183.
- [39] L.S. SHAPIRO, *Affine Analysis of Image Sequences*, Cambridge University Press, Cambridge, UK, 1995.
- [40] A. TERRAS, *Harmonic Analysis on Symmetric Spaces and Applications I*, Springer-Verlag, New York, 1985.
- [41] J. TURSKI, *Harmonic analysis on $SL(2, C)$ and projectively adapted pattern representation*, J. Fourier Anal. Appl., 4 (1998), pp. 67–91.

- [42] J. TURSKI, *Projective Fourier analysis in computer vision: Theory and computer simulations*, in Vision Geometry VI, R.A. Malter, A.Y. Wu, and L.J. Latecki, eds., SPIE 3168, Bellingham, WA, 1997, pp. 124–135.
- [43] J. TURSKI, *Projective Fourier analysis for patterns*, Pattern Recognition, 33 (2000), pp. 2033–2043.
- [44] J. TURSKI, *Geometric Fourier Analysis of the Conformal Camera*, The Departmental Seminar, Department of Mathematics, City University of Hong Kong, 2001.
- [45] J. TURSKI, *Projective Harmonic Analysis and Digital Image Processing*, The International Conference of Computational Harmonic Analysis, City University of Hong Kong, 2001.
- [46] J. TURSKI, *Projective Fourier analysis in computer vision: Mathematics for silicon retina sensors of active vision systems*, SIAM Conference: Mathematics for Industry—Challenges and Frontiers, Toronto, 2003.
- [47] P. VETTER, S.J. GOODBODY, AND D.M. WOLPERT, *Evidence for an eye-centered spherical representation of the visuomotor map*, J. Neurophysiol., 81 (1999), pp. 935–939.
- [48] M. YEASIN, *Optical flow in log-mapped image plane—A new approach*, IEEE Trans. Pattern Anal. Mach. Intell., 23 (2001), pp. 1–7.